

## Design and Synthesis of Alternating Regioregular Oligothiophenes/ Benzothiadiazole Copolymers for Organic Solar Cells

Fushun Liang,<sup>†,‡,§</sup> Jianping Lu,<sup>\*,‡</sup> Jianfu Ding,<sup>\*,†</sup> Raluca Movileanu,<sup>‡</sup> and Ye Tao<sup>‡</sup>

<sup>†</sup>Institute for Chemical Process and Environmental Technology (ICPET) and <sup>‡</sup>Institute for Microstructural Sciences (IMS), National Research Council of Canada (NRC), 1200 Montreal Road, Ottawa, ON K1A 0R6, Canada. <sup>§</sup>Current address: Department of Chemistry, Northeast Normal University, 5268 Renmin St., Changchun 130024, China.

Received May 4, 2009; Revised Manuscript Received July 6, 2009

**ABSTRACT:** Low-bandgap regioregular polythiophene derivatives, PTh<sub>6</sub>BTD, PTh<sub>8</sub>BTD, and PTh<sub>4</sub>TTBTD, were synthesized through Stille coupling reaction. These are alternating copolymers of an electron-deficient benzothiadiazole unit and oligothiophene units including hexathiophene, octathiophene, and thieno[3,2-*b*]thiophene-bridged quarterthiophene, respectively. The polymers are soluble in halogenated solvents such as *o*-dichlorobenzene, affording good processability in solar cell fabrication. Meanwhile, the synthesized alternating copolymers show much broader absorption than P3HT, covering the spectral region from 350 to 800 nm. DSC analysis showed that all three polymers readily crystallized, indicating highly ordered intermolecular packing, which is beneficial for achieving higher charge carrier mobility. Bulk-heterojunction solar cells using 1:1 w/w PTh<sub>*n*</sub>BTD:PC<sub>61</sub>BM ([6,6]-phenyl C<sub>61</sub>-butyric acid methyl ester) blends as the photovoltaic active layers were fabricated and characterized. Best power conversion efficiency of 1.7% was obtained from PTh<sub>8</sub>BTD-based devices under a simulated AM 1.5 G solar irradiation of 100 mW/cm<sup>2</sup>.

### Introduction

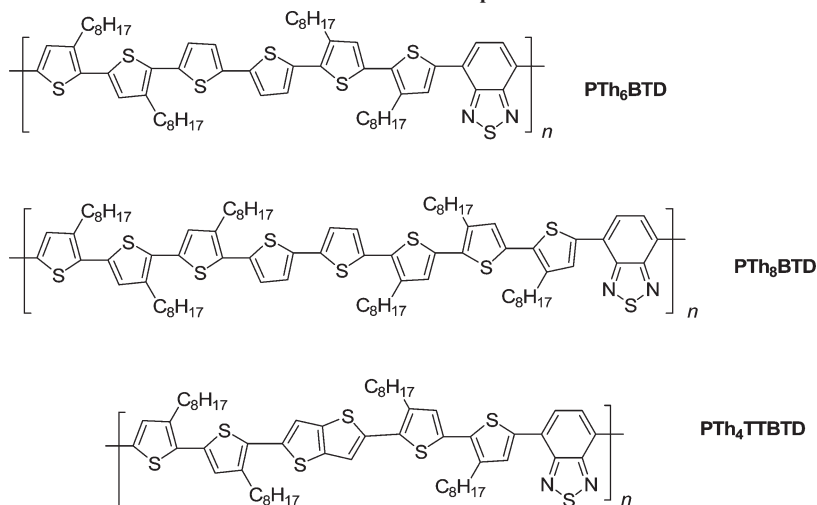
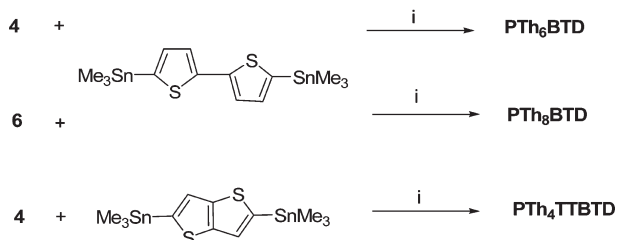
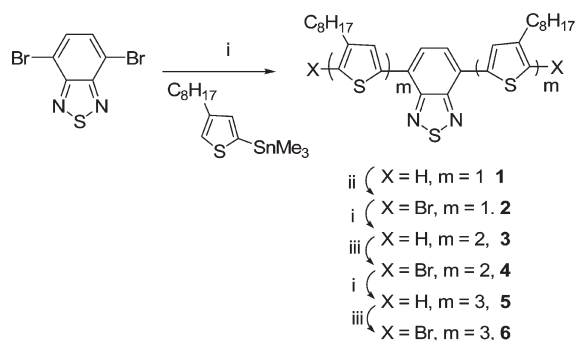
Despite facing challenges in long-term stability,<sup>1</sup> organic solar cells based on conjugated polymers and soluble fullerene derivatives have attracted a great deal of attention due to their solution processability, mechanical flexibility, and the potential for low-cost large-area manufacturing.<sup>2</sup> Recently, power conversion efficiencies in the 5% range have been reported independently by several groups based on poly(3-hexylthiophene)/[6,6]-phenyl C<sub>61</sub> butyric acid methyl ester (P3HT:PC<sub>61</sub>BM) bulk heterojunction (BHJ) solar cells.<sup>3–6</sup> Although P3HT is one of the most promising materials ever tested in polymeric solar cells, the mismatch between its relatively large band gap (2.0 eV) and the energy distribution of the solar spectrum leads to insufficient light absorption and limits the further improvement in the power conversion efficiency. Hence, it is necessary to lower the bandgap to move the absorption toward longer wavelengths. In this regard, low-bandgap polymers based on internal electron donor–acceptor (D–A) interaction have been developed. For instance, in 2006, Inganaes et al. reported low-bandgap alternating fluorene copolymers containing electron-withdrawing thioxaline;<sup>7</sup> Muehlbacher presented a copolymer of cyclopentadithiophene and 2,1,3-benzothiadiazole with a low bandgap of 1.73 eV;<sup>8</sup> and more recently, Leclerc and co-workers developed a low-bandgap poly(2,7-carbazole) derivative demonstrating a power conversion efficiency of 3.6% when blended with PC<sub>61</sub>BM as the photovoltaic (PV) active layer, and the efficiency was further improved to 6.1% after device optimization.<sup>9</sup>

On the other hand, due to strong interchain interaction in the solid state, some representative polythiophene systems like poly(3-hexylthiophene) (P3HT),<sup>3,5</sup> polyterthiophene (PTT),<sup>10</sup>

polyquarterthiophene (PQT),<sup>11</sup> and poly(2,5-bis(3-alkylthiophen-2-yl)thieno[3,2-*b*]thiophene) (PBTT)<sup>12</sup> show high charge carrier mobility, which is a very attractive feature and critically important for high-performance solar cells. Our strategy to develop low-bandgap polymers with high charge carrier mobility is to introduce a frequently used electron-deficient 2,1,3-benzothiadiazole (BTD) unit into the polythiophene main chain to lower the bandgap and to increase the number of thiophene rings in the oligothiophene segments for better interchain packing and solubility. With these in mind, 2,1,3-benzothiadiazole-cored regioregular oligothiophene monomers were designed and synthesized. Our recent work demonstrated that these oligothiophene monomers can be used as novel building blocks to construct crystalline polymeric materials for solar cell applications via copolymerization with other  $\pi$ -conjugated compounds such as indolo[3,2-*b*]carbazole.<sup>13</sup> In this work, these oligothiophenes were copolymerized with 5,5'-bis(stannyl)-2,2'-bithiophene or 2,5-bis(stannyl)thieno[3,2-*b*]thiophene via Stille reaction, resulting in three crystalline alternative copolymers, PTh<sub>6</sub>BTD, PTh<sub>8</sub>BTD, and PTh<sub>4</sub>TTBTD, as shown in Scheme 1. The length of the oligothiophene unit varied from 6 to 8 thiophene rings and thieno[3,2-*b*]thiophene-bridged 4 thiophene rings. To our knowledge, there are a few examples in the literature on the low-bandgap copolymers consisting of oligothiophenes and electron acceptors (quinoxaline,<sup>14</sup> oxadiazole,<sup>15</sup> benzothiadiazole,<sup>16</sup> or thiazolothiazole<sup>17</sup>). However, the maximum number of thiophene rings in the oligothiophene segments is no more than 4. Some of these polymers exhibited poor solubility in common organic solvents due to the lack of enough amount of alkyl side chains, and some polymers were synthesized via the oxidative polymerization method, in which the oxidant needs to be removed. In the previous work on the copolymers of oligothiophenes and benzothiadiazole, the best efficiency achieved was less than 1%.<sup>16</sup>

\*To whom all correspondence should be addressed: Ph (613)990-1651; Fax (613)990-0202; e-mail Jianping.Lu@nrc-cnrc.gc.ca, Jianfu.Ding@nrc-cnrc.gc.ca.

## Scheme 1. Chemical Structures Reported in This Work

Scheme 2. Synthetic Routes toward Copolymers PTh<sub>6</sub>BTD, PTh<sub>8</sub>BTD, and PTh<sub>4</sub>TTBTD<sup>a</sup>

<sup>a</sup> Reagents and conditions: (i) Pd(PPh<sub>3</sub>)<sub>4</sub>, toluene, Ar, 110 °C; (ii) NBS, CH<sub>2</sub>Cl<sub>2</sub>, rt; (iii) NBS, CH<sub>2</sub>Cl<sub>2</sub>, -10 °C.

In this paper, we present the synthesis of PTh<sub>6</sub>BTD, PTh<sub>8</sub>BTD, and PTh<sub>4</sub>TTBTD, followed by a detailed discussion on their optical, thermal, electrochemical, and photovoltaic properties, and demonstrate that with rational design of the substitution pattern of the substituents, low-bandgap semiconducting polymers with both high crystallinity and good solubility can be obtained. The initial study of the bulk-heterojunction solar cells using 1:1 w/w PTh<sub>8</sub>BTD:PC<sub>61</sub>BM blend as the PV active layer showed a power conversion efficiency of 1.7% under a simulated AM 1.5 G solar irradiation at 100 mW/cm<sup>2</sup>.

## Results and Discussion

**Synthesis.** Two key monomers **4** and **6**, dibrominated oligothiophenes incorporating benzothiadiazole in the center, were prepared in a divergent method from 4,7-dibromobenzothiadiazole via a repetitive Stille coupling and NBS bromination procedure (Scheme 2). We also attempted to synthesize quarterthiophene end-capped benzothiadiazole from

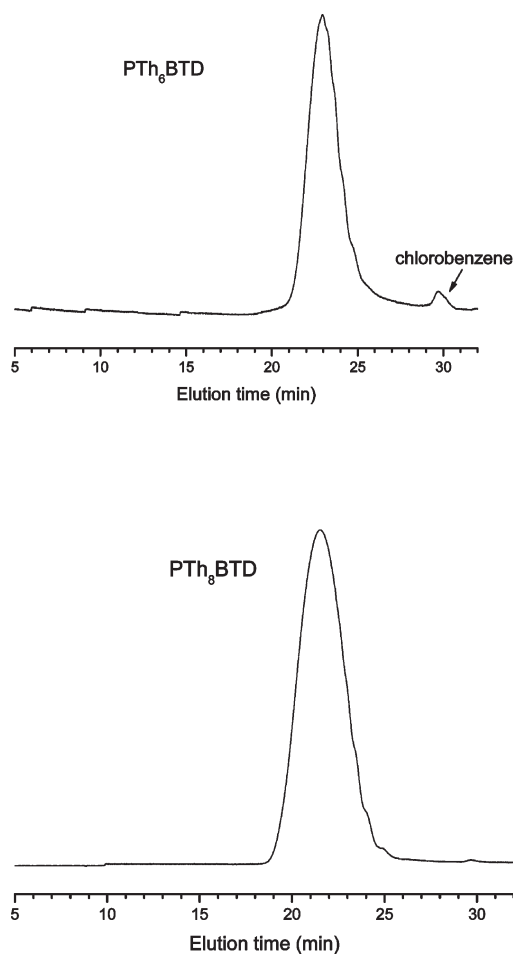


**Figure 1.** GPC curves of polymers PTh<sub>6</sub>BTD and PTh<sub>8</sub>BTD. PTh<sub>6</sub>BTD was first dissolved in chlorobenzene and then diluted with THF.

compound **6** but failed due to the purification problem. It is worth pointing out that the bromination condition was different for each cycle in order to get high bromination yield at the desired position. For example, 4,7-dibromo-2,1,3-benzothiadiazole was synthesized using liquid Br<sub>2</sub> as the bromination agent in 47% HBr solution with refluxing, while 4,7-bis(4-octyl-2-thienyl)-2,1,3-benzothiadiazole was readily brominated with *N*-bromosuccinimide (NBS) at room temperature

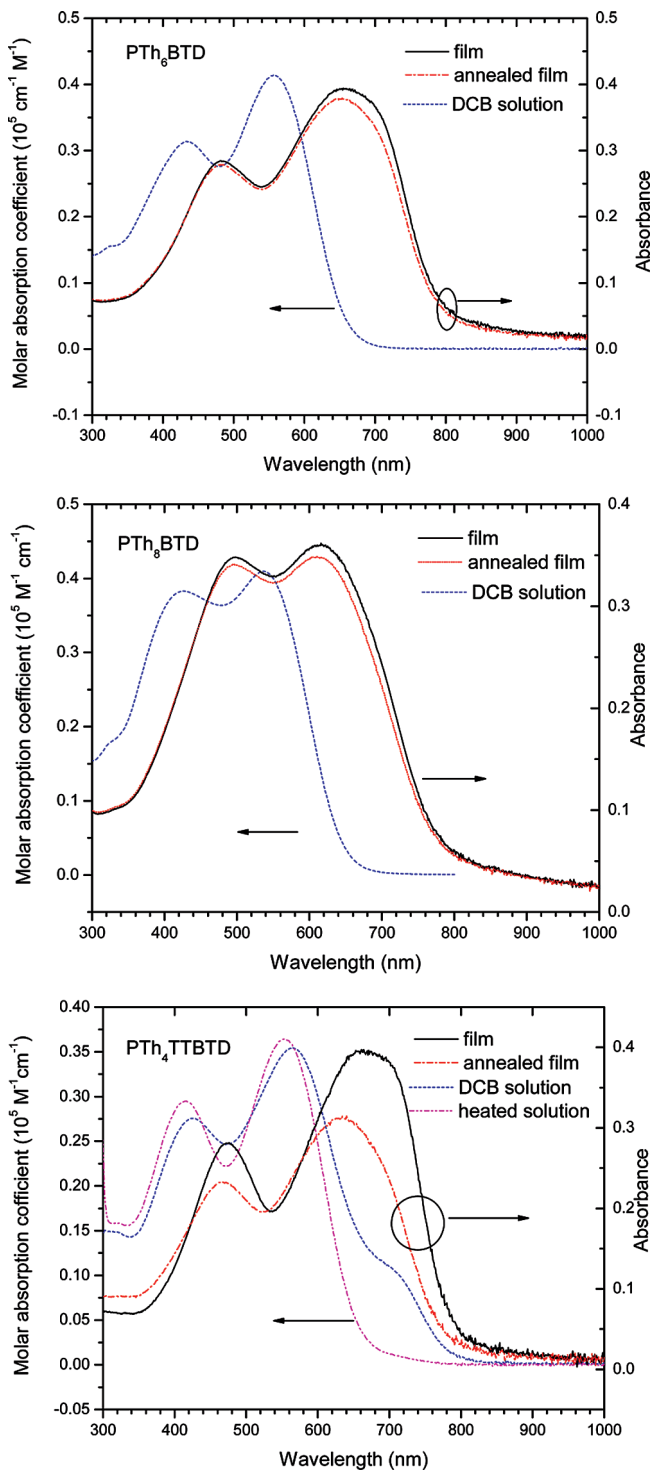


**Figure 2.** Absorption spectra of polymers PTh<sub>6</sub>BTD, PTh<sub>8</sub>BTD, and PTh<sub>4</sub>TTBTD in 1,2-dichlorobenzene solution and in solid film state (50 nm thick). The annealing temperatures for PTh<sub>6</sub>BTD, PTh<sub>8</sub>BTD, and PTh<sub>4</sub>TTBTD films are 120, 100, and 200 °C, respectively.

in the presence of silica gel as a catalyst. In contrast, the bromination of 4,7-bis(3,4',4''-trioctyl-2,2':5',2''-terthiophen-5-yl)-2,1,3-benzothiadiazole should be performed under even milder condition, such as at -10 °C. Otherwise, bromination would also occur at other positions, leading to the formation of a mixture that is difficult to purify.

All three polymers PTh<sub>6</sub>BTD, PTh<sub>8</sub>BTD, and PTh<sub>4</sub>TTBTD were successfully synthesized by Stille coupling between 5,5'-bis(trimethylstannyl)-2,2'-bithiophene or

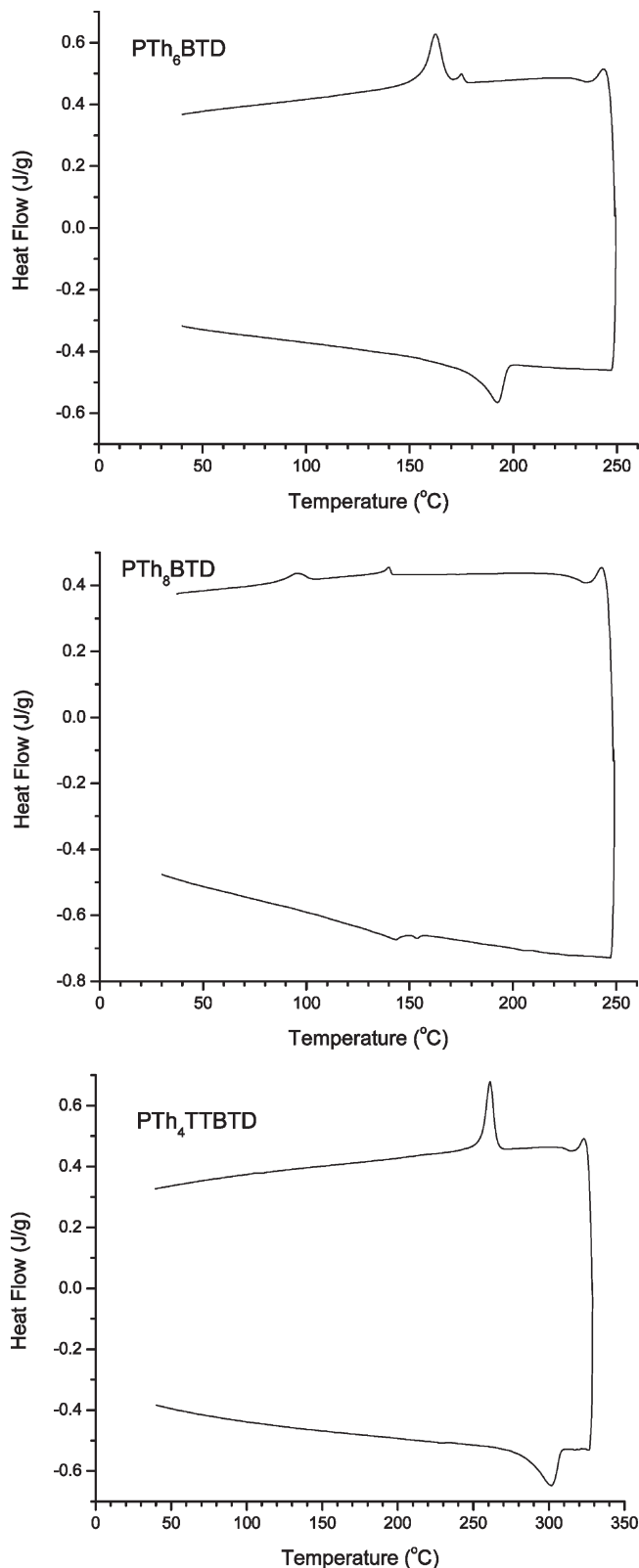


**Figure 3.** Second scan DSC curves of PTh<sub>6</sub>BTD and PTh<sub>8</sub>BTD. PTh<sub>4</sub>TTBTD at a heating/cooling rate of 10 °C under nitrogen.

2,5-bis(stannyl)thieno[3,2-*b*]thiophene and appropriate dibromo compounds in anhydrous toluene at 110 °C for 36 h.<sup>18</sup> Since the palladium catalyst is quite sensitive to oxygen and light, the polymerization reaction was run in the dark using a standard Schlenk technique. To increase the stability of the polymers, end-capping reactions were performed using

**Table 1. Physical Properties of Oligothiophenes–Benzothiadiazole Copolymers**

	$\lambda_{\text{max}}^{\text{abs}}$ [nm] <sup>a</sup>	optical gap [eV] <sup>b</sup>	$E_{1/2}^{\text{ox}}$ [V] <sup>c</sup>	$E_{1/2}^{\text{red}}$ [V] <sup>c</sup>	HOMO [eV] <sup>c</sup>	LUMO [eV] <sup>c</sup>	energy gap [eV] <sup>d</sup>	$T_m$ [°C] <sup>e</sup>
PTh <sub>6</sub> BTD	556	1.78	1.14	-1.10, -1.45	-5.26	-3.37	1.89	192
PTh <sub>8</sub> BTD	537	1.82	1.16	-1.11, -1.49, -1.70	-5.23	-3.30	1.93	143, 154
PTh <sub>4</sub> TTBTD	554 <sup>f</sup>	1.75	0.93	-1.29, -1.66	-5.03	-3.13	1.90	302

<sup>a</sup> Measured in 1,2-dichlorobenzene. <sup>b</sup> Estimated from the absorption edge of DCB solutions. <sup>c</sup> Determined by CV measurements. <sup>d</sup> Energy gap = HOMO – LUMO. <sup>e</sup> Determined by differential scanning calorimeter from remelt after cooling with a heating rate of 10 °C/min under N<sub>2</sub>. <sup>f</sup> Estimated from hot DCB solution.

bromobenzene and 2-stannylthiophene. The polymers were purified through Soxhlet extraction in refluxing acetone for 12 h and then in hexane for an additional 12 h to remove oligomers. PTh<sub>4</sub>TTBTD was further extracted with THF. Finally, high-molecular-weight polymers were extracted with chlorobenzene, concentrated, and precipitated in methanol. Black fibers for three polymers (PTh<sub>6</sub>BTD, PTh<sub>8</sub>BTD, and PTh<sub>4</sub>TTBTD) were obtained in moderate yields of 49%, 63%, and 45%, respectively. PTh<sub>8</sub>BTD was soluble in refluxing toluene, and no polymer precipitated out of solution during polymerization. As a result, high-molecular-weight PTh<sub>8</sub>BTD with narrow polydispersity was obtained in relatively higher yield. As shown in Figure 1, GPC analysis (gel permeation chromatography) showed that the number-average molecular weight ( $M_n$ ) of polymer PTh<sub>8</sub>BTD reached as high as 32 000 ( $M_w/M_n = 1.25$ ). On the contrary, polymers PTh<sub>6</sub>BTD and PTh<sub>4</sub>TTBTD precipitated out during polymerization due to their rigid backbone and hence lower solubility in refluxing toluene, leading to low molecular weights and reaction yields. The  $M_n$  of PTh<sub>6</sub>BTD only reached 8200 ( $M_w/M_n = 1.39$ ). The molecular weight of PTh<sub>4</sub>TTBTD cannot be measured on our GPC because of its extremely low solubility in the eluent (THF).

**Optical Property.** Figure 2 shows the UV–vis absorption spectra for polymers PTh<sub>6</sub>BTD, PTh<sub>8</sub>BTD, and PTh<sub>4</sub>TTBTD in solution and solid state, respectively. The dichlorobenzene solutions of all three polymers show broad absorption bands covering from 350 to 650 nm. The peak maxima located at ~550 nm arise from the intramolecular charge-transfer (ICT) transition.<sup>19</sup> These absorption maxima are accompanied by a strong absorption band at shorter wavelength (~425 nm) corresponding to the  $\pi$ – $\pi^*$  transition of the oligothiophene units.<sup>20</sup> The absorption shoulder peak at ~697 nm for PTh<sub>4</sub>TTBTD solution can be ascribed to the formation of polymer interchain aggregates because this absorption peak disappears upon heating.<sup>21</sup> Figure 2 also shows the absorption spectra of polymer thin films spin-cast from dichlorobenzene solution using a slow solvent evaporation process.<sup>5</sup> Compared with the solution absorption spectra, all three polymers showed pronounced peak broadening and red shifts of > 100 nm of absorption edges upon forming thin films. This phenomenon is attributed to the planarization of aryl rings and the presence of strong interchain interaction in the solid state.<sup>22</sup> It seems that the increase in the polymer backbone rigidity from PTh<sub>8</sub>BTD to PTh<sub>6</sub>BTD and PTh<sub>4</sub>TTBTD resulted in more pronounced interchain interaction, leading to more broadening of the absorption peaks. It is interesting to point out that the thin films of the three polymers showed slightly blue-shifted and reduced absorption upon annealing. This behavior is in sharp contrast to P3HT, which shows increased and red-shifted absorption upon annealing.<sup>6</sup> The polymers synthesized here are quite similar to P3HT, except that an electron-deficient moiety was incorporated into the main-chain structure. However, their optical properties are quite different from that of P3HT, indicating that the introduction of D–A structure in the polymer backbone has a strong impact on the interchain interaction.

**Thermal Properties.** The thermal properties of the polymers were investigated by differential scanning calorimetry (DSC). DSC analysis reveals that all three polymers are crystalline materials and have a strong tendency to crystallize, as evidenced by the appearance of the crystallization peaks in the DSC cooling scan and the absence of apparent glass transition in the heating scan. This property is beneficial for applications in organic solar cells since a highly ordered heterojunction nanostructure enhanced by the crystallization of the polymer in a PV active layer is desirable for charge separation and transport.<sup>3,23</sup> As can be seen from Figure 3, the increase of the benzothiadiazole content in the polymer backbone from PTh<sub>8</sub>BTD to PTh<sub>6</sub>BTD and PTh<sub>4</sub>TTBTD leads to monotonic increase in both the polymer melting point and melting enthalpy. It is worth pointing out that when the bithiophene moieties in polymer PTh<sub>6</sub>BTD was fused to become thieno[3,2-*b*]thiophene in polymer PTh<sub>4</sub>TTBTD, the melting point increased by 109 °C. This indicates that the thieno[3,2-*b*]thiophene moiety significantly increased the backbone rigidity and enhanced the interchain interaction. Perhaps, this is one of the reasons why thieno[3,2-*b*]thiophene semiconducting copolymers exhibited superior performance in organic transistors.<sup>24</sup>

**Electrochemical Properties.** To investigate the electrochemical properties of the synthesized polymers and estimate their HOMO and LUMO energy levels, cyclic voltammetry (CV) measurement was carried out in a three-electrode cell under Ar using 0.1 M Bu<sub>4</sub>NPF<sub>6</sub> in anhydrous CH<sub>3</sub>CN as the supporting electrolyte. A Pt disk (1 mm diameter), a Pt wire (0.5 mm diameter), and a silver wire (2 mm diameter) served as the working electrode, counter electrode, and quasi-reference electrode, respectively. Polymers were coated onto the working electrode from dichlorobenzene solution. Prior to the CV measurement, the Ag quasi-reference electrode was first calibrated using a ferrocene/ferrocenium (Fc/Fc<sup>+</sup>) redox couple (0.35 V vs Ag/AgCl)<sup>25</sup> as an external standard and was found to be -0.02 V vs SCE. Therefore, the LUMO and HOMO energy levels of the polymers can be estimated using the following empirical equations:  $E_{\text{HOMO}} = E_p' + 4.38$  eV and  $E_{\text{LUMO}} = E_n' + 4.38$  eV, respectively, where  $E_p'$  and  $E_n'$  are the onset potentials for oxidation and reduction relative to the Ag quasi-reference electrode, respectively. The results are summarized in Table 1, and the cyclic voltammograms are shown in Figure 4. All three polymers underwent reversible cathodic reduction and anodic oxidation, and the CV curves remained almost unchanged after successive multiple potential scans, indicating high stability of the materials for both hole and electron injection. For comparison purposes, the CV curve of widely used r,r'-P3HT was also included in Figure 4. As can be seen from Figure 4, all three polymers show additional redox pairs in the n-doping process owing to the presence of the electron-withdrawing benzothiadiazole units in the polymer backbone, leading to narrower energy gaps than P3HT. Meanwhile, the HOMO energy levels of both PTh<sub>6</sub>BTD and PTh<sub>8</sub>BTD remain low at ~5.25 eV, which are important for achieving large open-circuit voltage ( $V_{\text{oc}}$ ) and high air stability. Surprisingly, the HOMO energy level of PTh<sub>4</sub>TTBTD is relatively high

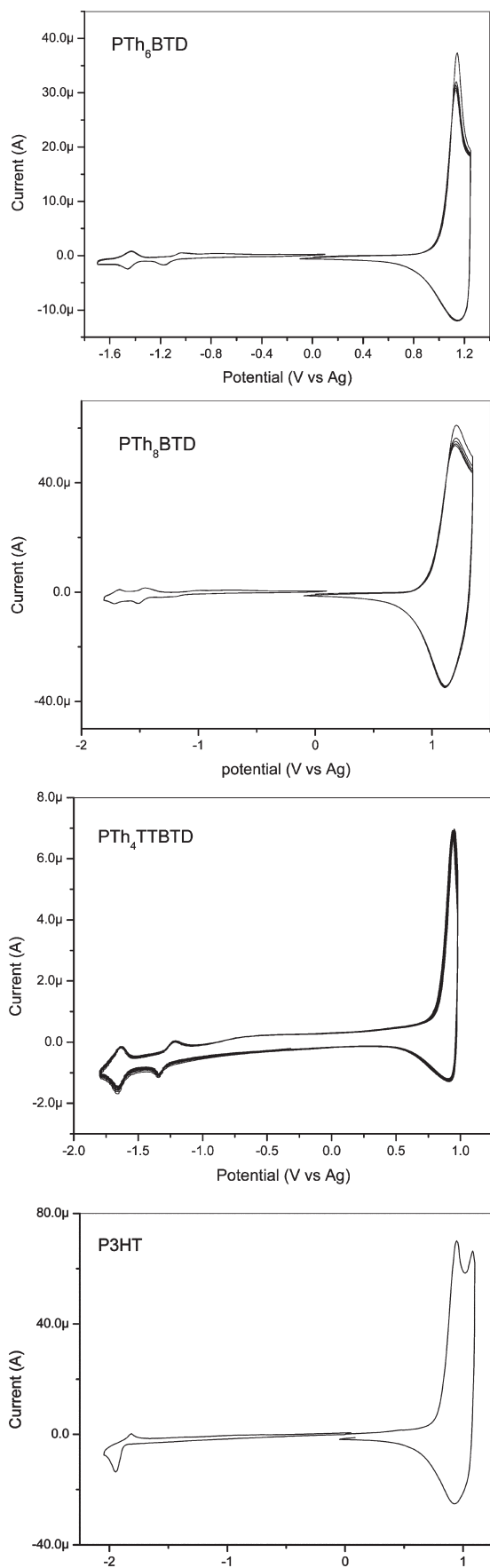


**Figure 4.** Cyclic voltammograms of PTh<sub>6</sub>BTD, PTh<sub>8</sub>BTD, PTh<sub>4</sub>TTBTD, and P3HT thin films on Pt electrode in 0.1 M Bu<sub>4</sub>NPF<sub>6</sub> acetonitrile solution at 50 mV/min.

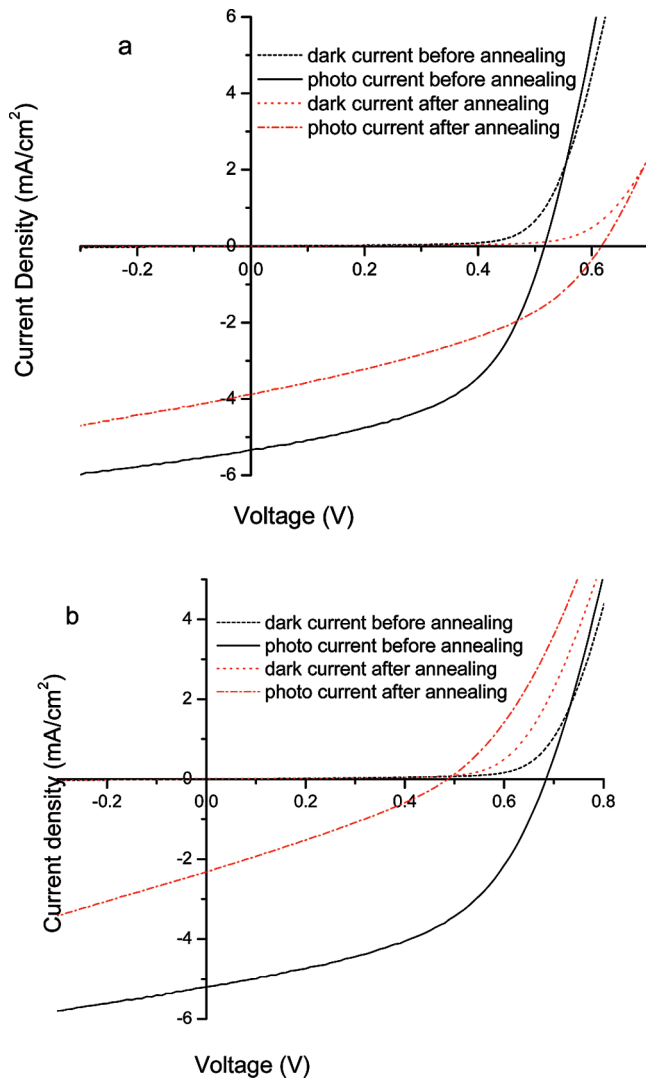


**Figure 5.** Current density–voltage characteristics of (a) PTh<sub>6</sub>BTD and (b) PTh<sub>8</sub>BTD solar cells under a simulated AM 1.5 solar irradiation of 100 mW/cm<sup>2</sup>.

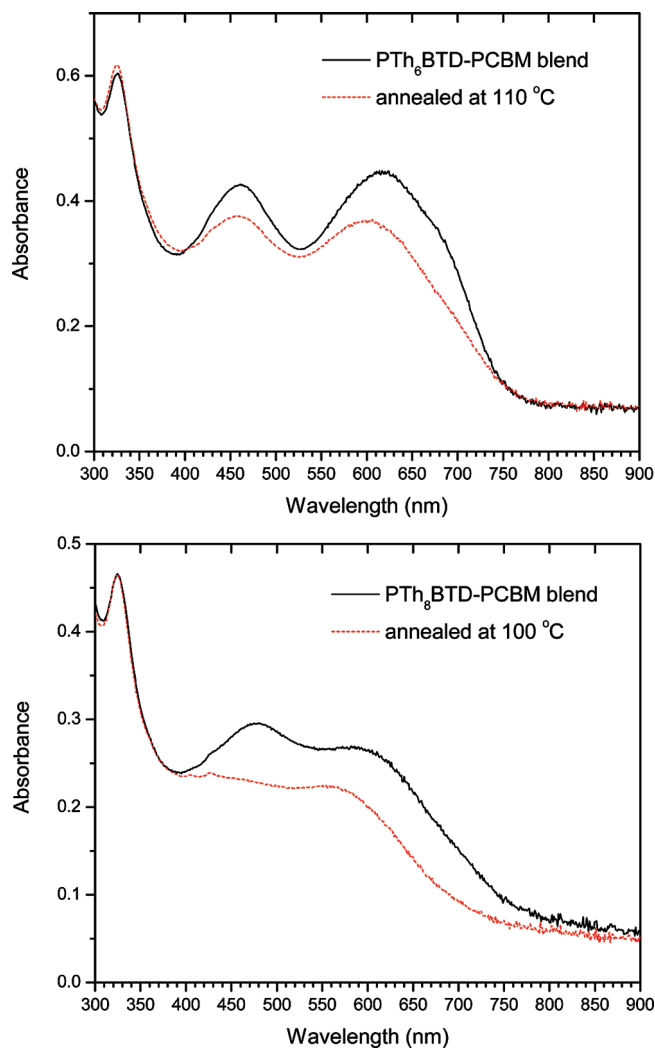
(5.03 eV) probably due to the more coplanar backbone conformation induced by the rigid thieno[3,2-*b*]thiophene moieties.

**Photovoltaic Properties.** The PV response of the synthesized low-bandgap polymers PTh<sub>6</sub>BTD, PTh<sub>8</sub>BTD, and PTh<sub>4</sub>TTBTD were investigated using bulk heterojunction PV cells with a device structure of ITO/PEDOT-PSS/PTh<sub>*n*</sub>BTD:PC<sub>61</sub>BM (1:1 w/w)/LiF (1 nm)/Al (120 nm). The active layer was spin-cast from dichlorobenzene solution using a slow solvent evaporation process.<sup>5</sup> Because of the very low solubility of PTh<sub>4</sub>TTBTD in dichlorobenzene at room temperature, it was difficult to get a dense and uniform film, and the resulting device was somewhat short-circuited. Figure 5 shows the current–voltage characteristics of the fabricated PV cells in the dark and under simulated AM 1.5 G solar irradiation at 100 mW/cm<sup>2</sup>. PTh<sub>8</sub>BTD-based devices have a  $V_{oc}$  of 0.68 V, higher than P3HT-based devices (~0.60 V). This can be explained by the higher oxidation potential of PTh<sub>8</sub>BTD. PTh<sub>6</sub>BTD has a HOMO energy level similar to PTh<sub>8</sub>BTD; however, to our surprise the  $V_{oc}$  of PTh<sub>6</sub>BTD-based devices is only 0.51 V, which is 0.17 V lower than that of PTh<sub>8</sub>BTD-based devices. The reason is not very clear at this moment. Our conjecture is that the relatively poor film quality of PTh<sub>6</sub>BTD due to its low solubility caused more

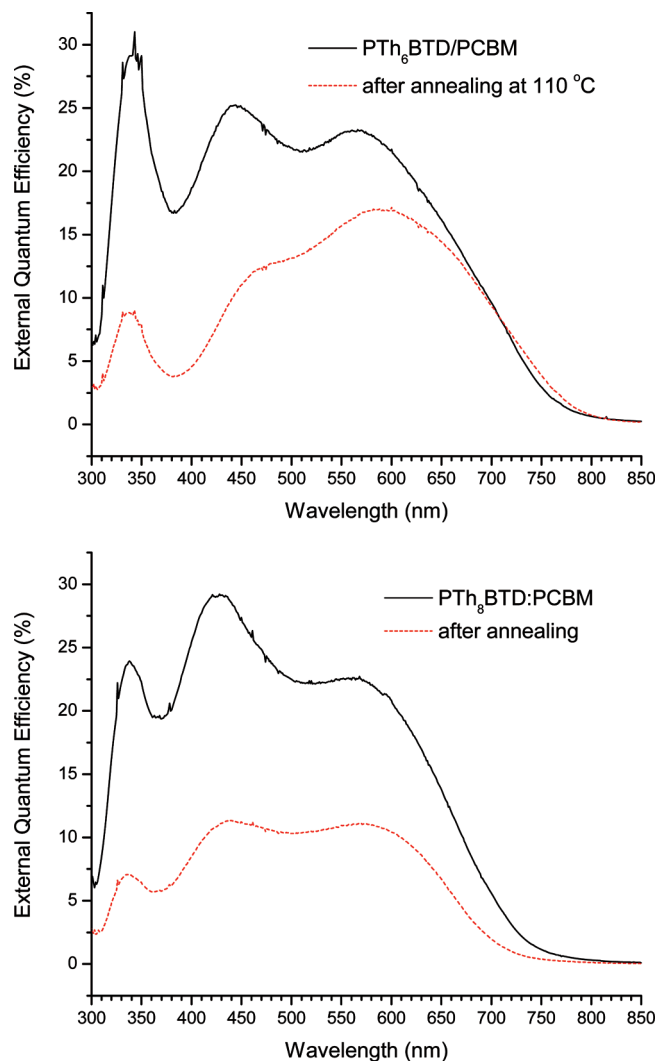
**Table 2. Summary of Device Performance for 1:1 PTh<sub>n</sub>BTD/PCBM (*n* = 6, 8) Based Solar Cells**

donor material	shunt resistance (kΩ cm <sup>2</sup> )	series resistance (Ω cm <sup>2</sup> )	<i>V</i> <sub>oc</sub> <sup>a</sup> (V)	<i>J</i> <sub>sc</sub> <sup>a</sup> (mA/cm <sup>2</sup> )	FF <sup>a</sup>	PCE <sup>a</sup> (%)
PTh <sub>6</sub> BTD	10.5 <sup>b</sup>	9.3 <sup>b</sup>	0.51 <sup>b</sup>	5.34 <sup>b</sup>	0.51 <sup>b</sup>	1.39 <sup>b</sup>
	15.6 <sup>c</sup>	17.3 <sup>c</sup>	0.61 <sup>c</sup>	3.88 <sup>c</sup>	0.40 <sup>c</sup>	0.95 <sup>c</sup>
PTh <sub>8</sub> BTD	14.6 <sup>b</sup>	13.5 <sup>b</sup>	0.68 <sup>b</sup>	5.20 <sup>b</sup>	0.49 <sup>b</sup>	1.73 <sup>b</sup>
	14.8 <sup>d</sup>	17.2 <sup>d</sup>	0.48 <sup>d</sup>	2.21 <sup>d</sup>	0.30 <sup>d</sup>	0.32 <sup>d</sup>

<sup>a</sup> Under simulated AM 1.5 solar illumination at an irradiation intensity of 100 mW/cm<sup>2</sup>. <sup>b</sup> For as-fabricated devices. <sup>c</sup> For devices annealed at 110 °C for 20 min. <sup>d</sup> For devices annealed at 100 °C for 20 min.

**Figure 6.** Absorption spectra of PTh<sub>n</sub>BTD/PCBM blends before and after thermal annealing.

energy loss during charge transport process. This is supported by the fact that the *V*<sub>oc</sub> of PTh<sub>6</sub>BTD-based devices was improved to 0.61 V upon annealing. PTh<sub>8</sub>BTD has a very good solubility in dichlorobenzene even at room temperature and can be readily cast into a dense film, leading to higher shunt resistance and a good fill factor. The device performance is summarized in Table 2. On the contrary to P3HT-based devices, thermal annealing of PTh<sub>n</sub>BTD-based devices did not improve the device performance. Indeed, the device series resistance increased after annealing, leading to the degradation of overall device performance. UV-vis absorption study showed that the absorption of the active layers blue-shifted and decreased in intensity after annealing, as displayed in Figure 6. This result is consistent with the change in the absorption spectra of polymer neat films upon annealing. We also carried out external quantum efficiency

**Figure 7.** External quantum efficiency spectra of 1:1 PTh<sub>n</sub>BTD/PCBM-based PV devices.

(EQE) measurement on our devices. As can be seen from Figure 7, the EQE curves of the devices are similar to the absorption spectra of the respective active layers except some small blue shifts in the polymer PV response peaks. EQE spectra clearly proved that the absorption of low-bandgap polymers PTh<sub>6</sub>BTD and PTh<sub>8</sub>BTD in the near-IR region (above 700 nm) contributed to the overall photocurrent generated by the devices under illumination. EQE measurement also confirmed that the photocurrent decreased after annealing.

## Conclusions

Polythiophene derivatives bearing electron-withdrawing benzothiadiazole moieties in the main chain were synthesized, and their optical, thermal, electrochemical, and photovoltaic properties were investigated in detail. The broad absorption and good

crystallinity demonstrate the potential of these polymers in solar cell applications. Bulk-heterojunction organic solar cells were fabricated with configuration of ITO/PEDOT-PSS/PTh<sub>8</sub>BTD:PCBM (1:1)/LiF/Al and examined under simulated AM 1.5 G solar irradiation. Preliminary results showed that PTh<sub>8</sub>BTD-based solar cells gave better performance with a PCE of 1.73%, a  $V_{oc}$  of 0.68 V, a short-circuit current ( $J_{sc}$ ) of 5.2 mA/cm<sup>2</sup>, and a fill factor (FF) of 0.49 in the unoptimized devices because of its high solar absorption, good solubility, and excellent film-forming property. This suggests that we have to make a compromise between solubility and high crystallinity when designing new polymeric materials for organic solar cell applications. In future work, we will focus on device optimization to further improve the power conversion efficiency, such as changing PC<sub>61</sub>BM loading ratio, optimizing active layer thickness, and replacing PC<sub>61</sub>BM with PC<sub>71</sub>BM for better absorption.

## Experimental Section

**Materials.** All reagents and solvents were purchased from Aldrich and Fisher Chemicals. Anhydrous tetrahydrofuran was distilled over sodium/benzophenone under Ar prior to use.

**Characterization.** NMR spectra were recorded on a 400 MHz Varian Unity Inova spectrometer using tetramethylsilane or trace chloroform in deuterium chloroform as internal references. Gel permeation chromatography (GPC, Viscotek TDA 302) was used for measuring the molecular weight and polydispersity index. UV-vis spectra were measured using a Varian Cary 50 Spectrometer. Differential scanning calorimetry (DSC) analysis was carried out on a TA Instruments DSC 2920 under nitrogen at a heating/cooling rate of 10 °C/min.

**Photovoltaic Device Fabrication and Testing.** Glass slides patterned with ITO (Colorado Concept Coatings LLC) were cleaned by sonicating sequentially in detergent, DI water, acetone, and isopropanol. The active area of each solar cell device was 5 × 7 mm<sup>2</sup>. Immediately prior to device fabrication, the ITO substrate was treated in a UV-ozone oven for 15 min. Thereafter, the ITO-coated slides were spin-coated (5000 rpm for 60 s) with a filtered (0.45 μm NYL with GMF syringe filter) aqueous suspension of poly(ethylene dioxythiophene) doped with poly(styrenesulfonic acid), PEDOT:PSS (Baytron P, H. C. Starck), and then baked at 120 °C under N<sub>2</sub> for 2 h. The resulting thin PEDOT:PSS layer was about 50 nm thick. A dichlorobenzene solution of polymer and PCBM (10.0 mg/mL each) was stirred at 50 °C overnight and then spun-cast on top of PEDOT:PSS at 600 rpm for 60 s. The film was kept in a Petri dish overnight. The thickness of the resulting film was found to be about 130 and 110 nm for PTh<sub>6</sub>BTD/PCBM and PTh<sub>8</sub>BTD/PCBM blend, respectively. The device fabrication was completed by the vacuum deposition of LiF (1 nm) and Al cathode (120 nm). The solar cells with no protective encapsulation were subsequently tested in air under simulated air mass (AM) 1.5 solar irradiation (100 mW/cm<sup>2</sup>, Sciencetech Inc., model SF150). Current-voltage ( $I-V$ ) characteristics were recorded using a computer-controlled Keithley 2400 source meter. External quantum efficiency (EQE) studies were performed using a Xe lamp on a Newport 90015832 monochromator with Newport motorized filter wheel system 74041. The probe beam was chopped at 30 Hz and the signal detected with Newport Merlin radiometry systems 70100 and a Stanford Research Systems SR570 lock-in amplifier.

**Monomer and Polymer Syntheses.** The dibromonated monomer **4** Th<sub>2</sub>BTD-2Br was synthesized from commercially available 2,1,3-benzothiadiazole via a divergent method according to our recent publication.<sup>13</sup> 2,5-Bis(trimethylstannyl)thieno[3,2-*b*]thiophene<sup>12</sup> and 5,5'-bis(trimethylstannyl)-2,2'-bithiophene<sup>26</sup> were prepared based on literature procedures.

4,7-Bis(3,4',4''-trioctyl-2,2':5',2''-terthiophen-5-yl)-2,1,3-benzothiadiazole (**5**, Th<sub>3</sub>BTD). Pd(PPh<sub>3</sub>)<sub>4</sub> (46 mg, 0.04 mmol) was

added to a solution of Th<sub>2</sub>BTD-2Br (2.14 g, 2.0 mmol) and trimethyl-(4-hexyl-2-thienyl)stannane (2.15 g, 6.0 mmol) in anhydrous DMF (15 mL). The mixture was stirred under argon for 24 h at 100 °C and then allowed to cool to room temperature. Saturated NaHCO<sub>3</sub> aqueous solution and hexanes (50 mL) were added. The aqueous layer was removed, and the organic layer was washed three times with distilled water. The organic layer was dried over magnesium sulfate, and the solvent was removed under a reduced pressure. The residue was purified by column chromatography on silica gel (eluent: hexane) to give compound **7** (2.16 g, 83%). <sup>1</sup>H NMR (400 MHz, C<sub>6</sub>D<sub>6</sub>, δ): 8.22 (s, 2H), 7.58 (s, 2H), 7.32 (s, 2H), 6.64 (s, 2H), 3.00 (t, 4H), 2.85 (t, 4H), 2.45 (t, 4H), 1.84 (m, 4H), 1.70 (m, 4H), 1.53–1.26 (m, 64H), 0.95–0.89 (m, 18H).

4,7-Bis(5''-bromo-3,4',4''-trioctyl-2,2':5',2''-terthiophen-5-yl)-2,1,3-benzothiadiazole (**6**, Th<sub>3</sub>BTD-2Br). A mixture of Th<sub>3</sub>-BTD (1.81 g, 1.39 mmol), *N*-bromosuccinimide (NBS) (0.50 g, 2.78 mmol), and silica gel (0.15 g) was dissolved in dichloromethane (30 mL) and stirred at –10 °C for 5.5 h. The reaction was quenched with water (100 mL) and then extracted with dichloromethane two times. The combined CH<sub>2</sub>Cl<sub>2</sub> solution was washed with water and dried over magnesium sulfate. Pure product was obtained by a silica gel column using hexane as eluent as a dark solid (1.54 g, 76%). <sup>1</sup>H NMR (400 MHz, C<sub>6</sub>D<sub>6</sub>, δ): 8.20 (s, 2H), 7.58 (s, 2H), 7.26 (s, 2H), 6.92 (s, 2H), 2.98 (t, 4H), 2.73 (t, 4H), 2.48 (t, 4H), 1.84 (m, 4H), 1.64 (m, 4H), 1.53–1.45 (m, 8H), 1.40–1.25 (m, 56H), 0.95–0.89 (m, 18H). <sup>13</sup>C NMR (100 MHz, C<sub>6</sub>D<sub>6</sub>, δ): 153.3, 143.4, 141.5, 141.3, 138.2, 136.3, 135.4, 133.0, 131.8, 131.3, 129.6, 127.7, 126.2, 125.7, 109.8, 32.6, 31.5, 31.4, 30.5, 30.42, 30.40, 30.3, 30.22, 30.17, 30.13, 30.10, 30.04, 30.02, 29.97, 23.46, 14.8, 14.7.

**General Procedure for the Preparation of Alternating Copolymers P(Th<sub>n</sub>BTD).** To a solution of appropriate dibromide (0.3 mmol) and 5,5'-bis(trimethylstannyl)-2,2'-bithiophene (0.3 mmol) in anhydrous toluene (6 mL), tetra(triphenylphosphine)-palladium(0) (7 mg, 0.006 mmol) was added in glovebox. The reaction mixture was stirred at ambient temperature for 5 min and then heated to reflux for 48 h. 2-(Trimethylstannyl)-thiophene (10 mg) was added, and 8 h later 2-bromothiophene (15 mg) was added and allowed to react for further 8 h. After the solution was cooled to 75 °C, chlorobenzene (10 mL) was added. The polymer was precipitated in methanol and collected by filtration. A dark purple fiberlike solid obtained was first washed with hexanes on Soxhlet extraction apparatus to remove low-molecular-weight oligomers and then extracted with chlorobenzene. The chlorobenzene solution was concentrated under reduced pressure and precipitated in methanol. The purified polymer was collected and dried in vacuum oven at 80 °C.

PTh<sub>6</sub>BTD. 157 mg, 49% yield. GPC:  $M_n$ : 8200,  $M_w/M_n$  = 1.39 (relative to polystyrene standards). Anal. Calcd for C<sub>62</sub>H<sub>78</sub>N<sub>2</sub>S<sub>7</sub>: C 69.22, H 7.31, N 2.60. Found: C 69.05, H 6.67, N 2.67.

PTh<sub>8</sub>BTD. 284 mg, yield 63%. GPC:  $M_n$  32 000; PDI 1.25. Anal. Calcd for C<sub>86</sub>H<sub>114</sub>N<sub>2</sub>S<sub>9</sub>: C 70.54, H 7.84, N 1.91. Found: C 70.65, H 7.47, N 2.07.

PTh<sub>4</sub>TTBTD. 142 mg, 45% yield. Anal. Calcd for C<sub>60</sub>H<sub>76</sub>N<sub>2</sub>S<sub>7</sub>: C 68.65, H 7.30, N 2.67. Found: C 68.34, H 7.15, N 2.84.

## References and Notes

- (1) (a) Jørgensen, M.; Norrman, K.; Krebs, F. C. *Sol. Energy Mater. Sol. Cells* **2008**, *92*, 686–714. (b) Thompson, B. C.; Fréchet, J. M. J. *Angew. Chem., Int. Ed.* **2008**, *47*, 58–77.
- (2) (a) Gunes, S.; Neugebauer, H.; Sariciftci, N. S. *Chem. Rev.* **2007**, *107*, 1324–1338. (b) Krebs, F. C. *Sol. Energy Mater. Sol. Cells* **2009**, *93*, 394–412. (c) Krebs, F. C. *Sol. Energy Mater. Sol. Cells* **2009**, *93*, 465–475. (d) Hoppe, H.; Sariciftci, N. S. *J. Mater. Chem.* **2006**, *16*, 45–61. (e) Krebs, F. C.; Jørgensen, M.; Norrman, K.; Hagemann, O.; Alstrup, J.; Nielsen, T. D.; Fyenbo, J.; Larsen, K.; Kristensen, J. *Sol. Energy Mater. Sol. Cells* **2009**, *93*, 422–441.

- (3) Ma, W.; Yang, C.; Gong, X.; Lee, K.; Heeger, A. J. *Adv. Funct. Mater.* **2005**, *15*, 1617–1622.
- (4) Kim, K.; Liu, J.; Namboothiry, M. A. G.; Carroll, D. L. *Appl. Phys. Lett.* **2007**, *90*, 163511.
- (5) Li, G.; Shrotriya, V.; Huang, J.; Yao, Y.; Moriarty, T.; Emery, K.; Yang, Y. *Nat. Mater.* **2005**, *4*, 864–868.
- (6) Kim, Y.; Cook, S.; Tuladhar, S. M.; Choulis, S. A.; Nelson, J.; Durrant, J. R.; Bradley, D. D. C.; Giles, M.; McCulloch, I.; Ha, C.-S.; Ree, M. *Nat. Mater.* **2006**, *5*, 197–203.
- (7) Zhang, F.; Mammo, W.; Andersson, L. M.; Admassie, S.; Andersson, M. R.; Inganaes, O. *Adv. Mater.* **2006**, *18*, 2169–2173.
- (8) Muehlbacher, D.; Scharber, M.; Morana, M.; Zhu, Z.; Waller, D.; Gaudiana, R.; Brabec, C. *Adv. Mater.* **2006**, *18*, 2884–2889.
- (9) (a) Blouin, N.; Michaud, A.; Leclerc, M. *Adv. Mater.* **2007**, *19*, 2295–2300. (b) Park, S. H.; Roy, A.; Beaupré, S.; Cho, S.; Coates, N.; Moon, J. S.; Moses, D.; Leclerc, M.; Lee, K.; Heeger, A. J. *Nat. Photonics* **2009**, *3*, 297–302.
- (10) Wu, Y. L.; Liu, P.; Gardner, S.; Ong, B. S. *Chem. Mater.* **2005**, *17*, 221–223.
- (11) Ong, B. S.; Wu, Y. L.; Liu, P.; Gardner, S. *J. Am. Chem. Soc.* **2004**, *126*, 3378.
- (12) McCulloch, I.; Heeney, M.; Bailey, C.; Genevicius, K.; Macdonald, I.; Shkunov, M.; Sparrowe, D.; Tierney, S.; Wagner, R.; Zhang, W.; Chabinyc, M.; Kline, R.; McGehee, M.; Toney, M. *Nat. Mater.* **2006**, *5*, 328–333.
- (13) Lu, J. P.; Liang, F.; Drolet, N.; Ding, J.; Tao, Y.; Movileanu, R. *Chem. Commun.* **2008**, 5315–5317.
- (14) Tsami, A.; Buennagel, T. W.; Farrell, T.; Scharber, M.; Choulis, S. A.; Brabec, C. J.; Scherf, U. *J. Mater. Chem.* **2007**, *17*, 1353–1355.
- (15) Levi, M. D.; Fisyuk, A. S.; Demadrille, R.; Markevich, E.; Gofer, Y.; Aurbach, D.; Pron, A. *Chem. Commun.* **2006**, 3299–3301.
- (16) (a) Bundgaard, E.; Krebs, F. C. *Macromolecules* **2006**, *39*, 2823–2831. (b) Bundgaard, E.; Krebs, F. C. *Sol. Energy Mater. Sol. Cells* **2007**, *91*, 1019–1025. (c) Bundgaard, E.; Shaheen, S. E.; Krebs, F. C.; Ginley, D. S. *Sol. Energy Mater. Sol. Cells* **2007**, *91*, 1631–1637.
- (17) Osaka, I.; Sauv e, G.; Zhang, R.; Kowalewski, T.; McCullough, R. D. *Adv. Mater.* **2007**, *19*, 4160–4165.
- (18) Farina, V.; Krishnamurthy, V.; Scott, W. J. *Org. React.* **1997**, *50*, 1–652.
- (19) Sonar, P.; Singh, S. P.; Sudhakar, S.; Dodalapur, A.; Sellinger, A. *Chem. Mater.* **2008**, *20*, 3184–3190.
- (20) Tour, J. M.; Wu, R. *Macromolecules* **1992**, *25*, 1901–1907.
- (21) Apperloo, J. J.; Janssen, R. A. J.; Malenfant, P. R. L.; Fr chet, J. M. J. *J. Am. Chem. Soc.* **2001**, *123*, 6916–6924.
- (22) Brown, P. J.; Thomas, D. S.; K hler, A.; Wilson, J. S.; Kim, J. S.; Ramsdale, C. M.; Sirringhaus, H.; Friend, R. H. *Phys. Rev. B: Condens. Matter Mater. Phys.* **2003**, *67*, 642031.
- (23) Lu, J.; Xia, P.; Lo, P.; Tao, Y.; Wong, M. *Chem. Mater.* **2006**, *18*, 6194–6203.
- (24) McCulloch, I.; Heeney, M.; Chabinyc, M.; DeLongchamp, D.; Kline, R. J.; C lle, M.; Duffy, W.; Fischer, D.; Gundlach, D.; Hamadani, B.; Hamilton, R.; Richter, L.; Salleo, A.; Shkunov, M.; Sparrowe, D.; Tierney, S.; Zhang, W. *Adv. Mater.* **2009**, *21*, 1091–1109.
- (25) Pommerehne, J.; Vestweber, H.; Guss, W.; Mahrt, R. F.; Bassler, H.; Porsch, M.; Daub, J. *Adv. Mater.* **1995**, *7*, 551–554.
- (26) Usta, H.; Lu, G.; Facchetti, A.; Marks, T. J. *J. Am. Chem. Soc.* **2006**, *128*, 9034–9035.